Proceedings of "Applications of Physics in Mechanical and Material Engineering" (APMME 2023)

Influence of Thermal Loads on the Microstructure and Mechanical Properties of Structural Steel

T. Domański[a,*], W. Piekarska[b], M. Sága[c], M. Kubiak[a], Z. Saternus[a] and Z. Ságová[c]

[a]*Department of Mechanical Engineering and Computer Science, Częstochowa University of Technology, Dąbrowskiego 69, 42-201 Częstochowa, Poland*
[b]*Faculty of Architecture, Civil Engineering and Applied Arts, University of Technology, Rolna 43, 40-555 Katowice, Poland*
[c]*Department of Applied Mechanics, University of Žilina, Univerzitná 1, 010 26 Žilina, Slovak Republic*

Doi: 10.12693/APhysPolA.144.300 *e-mail: tomasz.domanski@pcz.pl

In this work, the change in the mechanical and microstructural properties of the material exposed to elevated temperatures was investigated in order to determine the variable and temperature-dependent strength parameters. The article presents the results obtained during the uniaxial tensile test of the samples (including modulus of elasticity, yield strength, and tensile strength) under variable thermal conditions. The heating process took place in a modern furnace using T3 lamps in the temperature range up to 1100°C. The MTS extensometer was used for the measurement.

topics: heating, tensile tests, material properties, hot working steel

1. Introduction

Steel products with properties enabling operation at high temperatures have become available on the market in recent years due to the development of metallurgical and production technologies. Steel grade WCL/1.2343/X37CrMoV5-1 is widely used in various industrial sectors, including automotive, aerospace, and machine tools. Many manufacturers of cutting tools use it to produce high-quality, durable, and wear-resistant tools [1, 2]. This steel is used in the production of tools for processing light metal alloys, for hot stamping, and for the production of nuts, rivets, and screws. The stiffness and strength of steel elements may decrease as a result of operation at elevated temperatures, which plays a key role in designing the fire resistance of steel structures. The properties of materials at elevated temperatures are defined in international specifications for steel structures such as European Standard (EC3), American Specification (AISC Specification), and Australian Standard (AS 4100) [3]. However, the material properties at elevated temperatures in these specifications are based primarily on experimental data on normal-strength hot-rolled carbon steel.

Knowledge of the basic strength parameters of the material is important for technologists and structure designers [4–7]. The study of the mechanical and thermomechanical properties of the material is also important for numerical modelling [8]. Nowadays, numerical modelling is increasingly used at the initial stages of production. Reliable processing of appropriate material data increases the computational accuracy of discrete models.

2. Infrared radiant heating chamber

An infrared heating chamber Model E4 is used in experimental tests of rod heating. Figure 1 shows a diagram of the heating chamber. The heating chamber allows for very quick heating of elements using highly concentrated infrared energy. This energy is generated by two halogen lamps and focused on the axis of the furnace using four elliptical reflectors. From a cold start, the lamps reach 90% of the operating temperature within 3 s. The device allows to heat elements up to 1100°C [9, 10].

3. Measuring system

Universal testing machine Zwick/Roell Z100 with maximum load 100 kN and precision 1 N force/0.01 mm displacement (without extensometer, see Fig. 2) is used in the research [8].

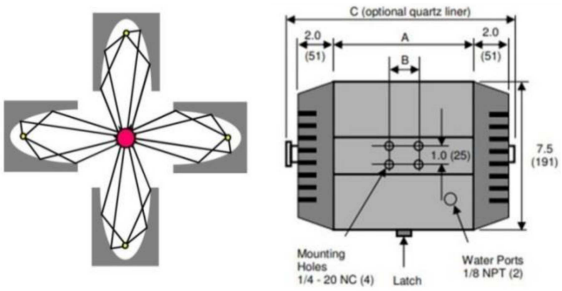

Fig. 1. Diagram of infrared heating chamber [9].

Fig. 2. The measurement system used in experimental tests.

TABLE I

The chemical composition of WCL/1.2343/X37CrMoV5-1 steel.

Element	C	Si	Mn	P
	0.33–0.41	0.80–1.20	0.25–0.50	max–0.030
Element	S	Cr	Mo	V
	max–0.030	4.80–5.50	1.10–1.50	0.30–0.50

The universal machine is coupled with a heating chamber that adjusts temperatures during the tensile test. The elongation measurement is carried out by determining the position of the movable cross-head and an additional MTS extensometer equipped with ceramic fingers that contact the tested sample inside the heating chamber during the measurement.

In order to determine the strength properties (Young's modulus, elasticity and yield strength, ultimate tensile strength), a series of static tensile

Fig. 3. Samples used in experimental tests.

Fig. 4. A set of samples obtained after experimental tests.

tests are carried out on samples with a circular cross-section and a threaded shank part (Fig. 3). The tests are performed for samples at the following temperatures: 20, 100, 200, 300, 400, and 600°C.

The samples are made of hot work tool steel — WCL/1.2343/X37CrMoV5-1. Table I shows the chemical composition of tested steel.

4. The true stress–strain curve

On the basis of tension diagrams for various temperatures, it is possible to develop a numerical (approximated) diagram for the tension of steel. Commercial strength analysis software requires the implementation of true stress–strain diagrams. Therefore, the experimentally obtained steel tension diagram should be transformed into a true stress–strain curve used by the software [11].

The value of true stress σ_{True} is determined on the basis of the actual stress (σ_{En}) diagram, obtained in the testXpert II program,

$$\sigma_{\mathrm{En}} = \frac{F}{A_o}, \qquad \sigma_{\mathrm{True}} = \frac{F}{A}, \tag{1}$$

where $A = A_o\, L_o/L$, and

$$\sigma_{\mathrm{True}} = \frac{F}{\mathrm{A}} = \frac{F\, L}{A_o L_o} = \frac{F}{A_o}\left(1 + \varepsilon_{\mathrm{En}}\right), \tag{2}$$

where F is forces [N], A — actual cross-sectional area [mm^2], A_o — initial cross-sectional area [mm^2], L — measurement length [mm], L_o — initial measurement length [mm], and $\varepsilon_{\mathrm{En}}$ — actual displacement.

Finally,

$$\sigma_{\mathrm{True}} = \sigma_{\mathrm{En}}\left(1 + \varepsilon_{\mathrm{En}}\right). \tag{3}$$

Determining true strain ($\varepsilon_{\mathrm{True}}$) on the basis of the real displacement ($\varepsilon_{\mathrm{En}}$) is performed as follows

$$\varepsilon_{\mathrm{En}} = \frac{\Delta L}{L_o} = \frac{L}{L_o} - 1,$$
$$\varepsilon_{\mathrm{True}} = \int_{L_o}^{L} \frac{\mathrm{d}L}{L} = \ln\left(\frac{L}{L_o}\right). \tag{4}$$

Therefore,

$$\varepsilon_{\mathrm{True}} = \ln\left(1 + \varepsilon_{\mathrm{En}}\right). \tag{5}$$

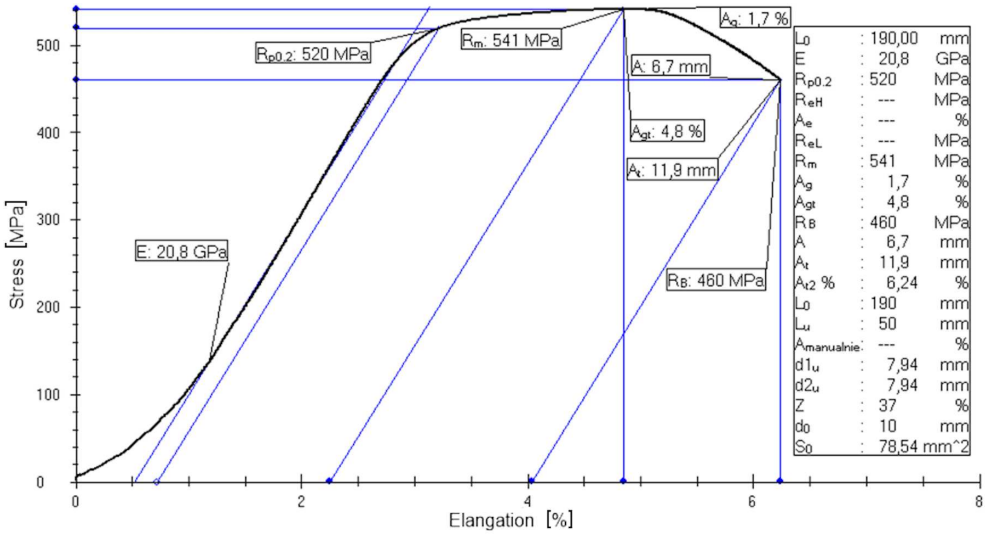

Fig. 5. Diagram of steel tension at temperature of 20°C with characteristic values.

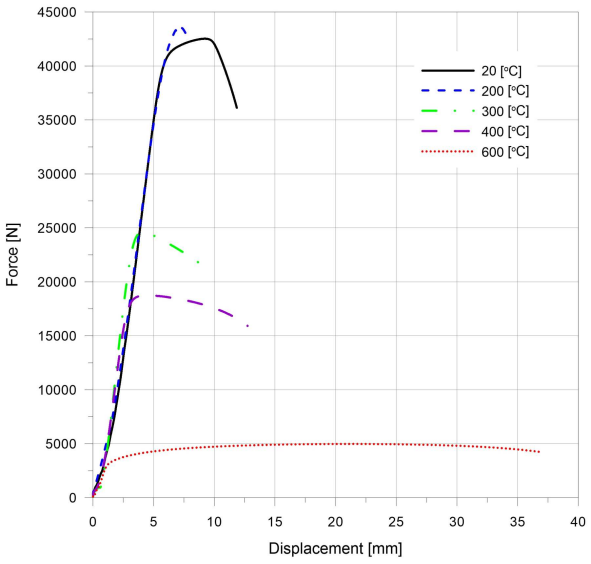

Fig. 6. Stress–displacement curves of WCL/1.2343 steel for different temperatures.

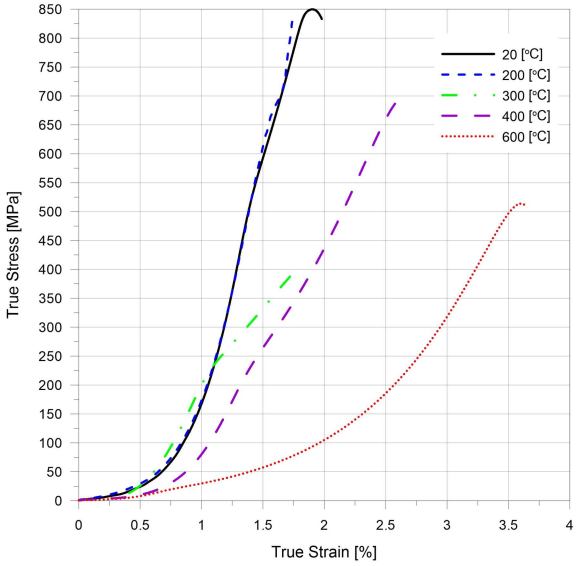

Fig. 7. True stress–strain diagrams for difference temperatures.

5. Experimental results

Figure 4 shows the sample scraps obtained after the tensile test. A quite significant difference in elongation can be noticed in the case of samples stretched at higher temperatures.

Figure 5 shows the actual tensile diagram obtained in the testXpert II program with marked strength values.

Table II shows the material properties obtained from the static tensile test.

Figure 6 shows the results of all tensile tests for 5 different temperatures. It can be observed that plasticity increases and the value of Young's modulus lowers at a higher temperature of the sample.

TABLE II

Material properties obtained of the experimental metods.

No.	T [°C]	E [GPa]	$R_{0.2}$ [MPa]	R_m [MPa]	A_o [%]
1.	20	21.0	518	541	6.24
2.	200	17.8	551	587	5.73
3.	300	25.0	305	313	5.10
4.	400	19.7	231	239	6.71
5.	600	6.26	43.8	63.4	19.42

Using the experimentally obtained strain diagrams (Fig. 6) and equations (3) and (5), it is possible to develop a true stress–true strain diagram (Fig. 7).

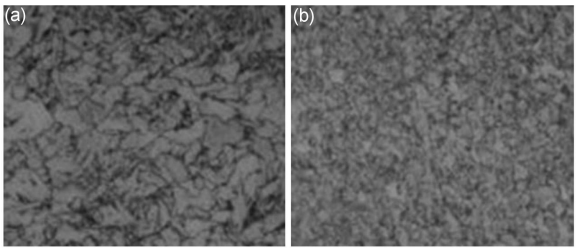

Fig. 8. Microstructure of the tested material for two selected temperatures (a) 20°C, (b) 600°C.

Figure 8 shows photos of the microstructure of two selected samples heated to 20°C (a) and 600°C (b).

6. Conclusions

In this work, a number of experimental tests are performed to determine the material properties of steel at various temperatures. These studies allowed the development of a discrete numerical model of the material, which can be used in computational simulations of analysed steel. Simulation results based on experimental tests increase computational accuracy.

Acknowledgments

The authors' work in this article was carried out as part of project 313011ASY4 by the University of Žilina "Strategic implementation of additive technologies to strengthen the intervention capacities of emergencies caused by the COVID-19 pandemic."

References

[1] Z. Guo, X. Wang, Y. Liu, Y. Liu, F. Li, *J. Constr. Steel Res.* **172**, 106174, (2020).

[2] X. Yan, Y. Xia, H.B. Blum, T. Gernay, *J. Constr. Steel Res.* **174**, 106299, (2020).

[3] H.-T. Li, B. Young, *Thin-Walled Struct.* **115**, 289 (2017).

[4] A. Su, Y. Sun, Y. Liang, O. Zhao, *Thin-Walled Struct.* **152**, 106723 (2020).

[5] P. Ptak, M. Pierzgalski, D. Cekus, K. Sokół, *Proc. Eng.* **177**, 175 (2017).

[6] F. Bárnik, M. Vaško, M. Sága, M. Handrik, A. Sapietová, *MATEC Web Conf.* 11, 01018 (2019).

[7] D. Wilczyński, I. Malujda, K. Talaśka, R. Dlugi, *Proc. Eng.* **177**, 411 (2017).

[8] T. Domański, W. Piekarska, Z. Saternus, M. Kubiak, S. Stano, *Materials* **15**, 3243 (2022).

[9] ChamberIR, E4 Data Sheet.

[10] ChamberIR, E4 User Manual.

[11] I. Faridmehr, M.H. Osman, A.B. Adnan, A.F. Nejad, R. Hodjati, M. Azimi, *Am. J. Civ. Eng. Archit.* **2**, 53 (2014).